Scripta METALLURGICA Vol. 19, pp. 499-504, 1985 Pergamon Press Ltd.
Printed in the U.S.A.

Solution Strengthening in Al-Zn
A Nuclear Magnetic Resonance Study

J. Th. M. De Hosson, U. Schlagowski*, O. Kanert*

Department of Applied Physics, Materials Science Centre, University of Groningen,
Nijenborgh 18, 9747 AG Groningen, The Netherlands.
*Institute of Physics, University of Dortmund, 4600 Dortmund 50, FRG.

(Received December 18, 1984)
(Revised January 28, 1985)

1. Introduction

The great strength of nuclear magnetic resonance is that the resonance signal is characteristic of a particular nucleus being studied. As a result, nuclear magnetic resonance can be used to measure properties which belong exclusively to the nuclei whose properties are of interest. Secondly, the surrounding of a nucleus may affect NMR properties like spin-lattice relaxation time. Accordingly, NMR can be used to study the environment of the nuclei providing microscopic information of atomic motions. In the following, we report of effects of dislocation motion in metals on the NMR spin-lattice relaxation time, from which microscopic observation about the dislocation dynamics can be obtained. Whenever a dislocation changes its position in the crystal, the surrounding atoms have also to move, thus causing time fluctuations of the quadrupolar field that dominates the observed spin-lattice relaxation behaviour.

We have concentrated on plastic deformation experiments with a constant strain rate $\dot{\varepsilon}$. This type of experiment is governed by Orowan's equation (1):

$$\dot{\varepsilon} = \phi b \rho_m \frac{L}{\tau_m} \quad , \tag{1}$$

assuming a thermally activated, jerky motion of mobile dislocations of density ρ_m. The motion may be considered to be jerky-like, if the actual jump time τ_j is small compared to the mean time of stay τ_m at an obstacle. In Eq. (1), ϕ denotes a geometrical factor, b symbolizes the magnitude of the Burgers vector and L is the mean jump distance between obstacles which are considered to be uniform. Clearly, alloying introduces extra barriers to the motion of dislocations. Therefore, during plastic deformation of a binary solid solution such as Al-1 at% Zn, moving dislocations are hindered in their glide plane by two types of obstacles: forest dislocations and solute atoms. The theory of obstacle strengthening can be complicated, and Nabarro (2)(3) has shown how the important features can be distinguished. Nevertheless, it has been recognized from the time of the earliest theories that it is difficult to estimate the segment length of a dislocation line that advances during plastic flow. NMR techniques can provide experimental information about the length of a moving dislocation line segment.

2. Theoretical Background

A few years ago, we showed that pulsed nuclear magnetic resonance is a useful tool to study dislocation dynamics in both ionic and metallic systems. It turned out that in principle three sets of microscopic information about the dislocation motion can be deduced from experiments: (i) the mean jump distance of moving dislocations; (ii) the mean time of stay between two consecutive jumps of mobile dislocations; (iii) the mobile dislocation density as a fraction of the total dislocation density.

The experimental method is essentially based on the interaction between nuclear electric quadrupole moments and electric field gradients at the nucleus. Around a dislocation in a cubic crystal the symmetry is destroyed and interactions between nuclear electric quadrupole moments and electric field gradients arise. Whenever a dislocation changes its position in the crystal, the surrounding atoms have also to move, thus causing time fluctuations of the quadrupolar spin Hamiltonian for spins with $I > 1/2$.

While deforming a sample with a constant strain rate $\dot{\varepsilon}$, the spin-lattice relaxation rate in a weak, rotating, applied field H_1 of the resonant nuclei is enhanced due to the motion of dislocations. The resulting expression for the relaxation rate induced by dislocation motion is given by:

0036-9748/85 $3.00 + .00

$$\left(\frac{1}{T_{1\rho}}\right)_D = \frac{A_Q}{H_1^2 + H_{L\rho}^2} \quad \frac{1}{\phi b L} \quad \dot{\varepsilon} \quad , \tag{2}$$

where A_Q depends on the mean-squared electric field gradient due to the stress field of a dislocation of unit length. $H_{L\rho}$ is the mean local field in the rotating frame, b is the magnitude of the Burgers vector, ϕ is a geometrical factor and L is the mean jump distance. A_Q and $H_{L\rho}^2$ can be determined separately from spin-echo NMR measurements. Hence, for a given plastic deformation rate $\dot{\varepsilon}$, the nuclear spin-lattice relaxation rate is proportional to the inverse of the mean jump distance L. Relationship (1) has been used to determine L as a function of strain. For detailed information on this method, reference should be made to our review article (4). The mean jump distance will be analyzed in terms of Friedel and Mott-Nabarro 'statistics'. The word 'statistics' has been quoted from the review article by Kocks et al. (8), although this expression does not come from the original source (2).

3. Experimental

To avoid skin effect distortion of the NMR signal, the NMR experiments were carried out on rectangular foils of size 27 mm x 12 mm x 40 m. Polycrystalline samples with a grain size of the order of 100-200 µm were used. The starting material for the samples was (a) 5N aluminium and (b) 5N Al: 1 at% Zn. After homogenizing procedure at 550 °C for 2.5 days, the material was rolled out to thin foils with a thickness of about 40 m and has been cut by spark erosion to the sample size given above.

Then, the samples (a) consisting of ultrapure aluminium were annealed a second time at 290 °C for 1 hr. The aluminium-zinc alloy was annealed at 550 °C for 1 hr , quenched in water for 3.5 hrs at 360 °C and quenched in ice water.

In the NMR experiment, the sample under investigation is plastically deformed by a servo-hydraulic tensile machine (Zonic Technical Lab. Inc., Cincinnati) of which the exciter head XCI TE 1105 moves a driving rod with a constant velocity. The movement is controlled by a digital function generator which serves the master controller of the exciter head.

While the specimen was deforming, ^{27}Al nuclear spin-relaxation measurements were carried out by means of a Bruker pulse spectrometer SXP 4-100 operating at 15.7 MHz corresponding to a magnetic field of 1.4 T controlled by an NMR stabilizer (Bruker B-SN 15).

The NMR head of the spectrometer consisting of a flat rf coil of silver and tuning elements and the frames in which the rod moves formed together a unit which was inserted between the pole pieces of the electro-magnet of the spectrometer. During the deformation experiments, the acting load and the resulting plastic deformation are measured separately and simultaneously. Information of the experimental set-up can be found in (5).

The NMR experiments discussed here were carried out at T=77 K. At such a low temperature nuclear spin relaxation effects because of diffusive atomic motions are negligible. The self-diffusion coefficient as well as the impurity diffusion of Zn in aluminium, are published in the literature (6)(7). Use of these data in the Einstein-Smoluchowsky relation (connecting the diffusion coefficient D with the mean time of stay of an atom between two diffusion jumps), proves that Al and Zn atoms are actually immobile at 77 K. The correlation times for diffusive atomic jumps are much larger than typical values of the waiting time of mobile dislocations, which are about 10^{-4} s for $\dot{\varepsilon} \simeq 1\ s^{-1}$. Consequently, an observable contribution of diffusive atomic motions to the measured spin-lattice relaxation rate does not occur.

Transmission electron micrographs were taken by using a JEM 200 CX. Disk-type specimens were obtained from the deformed foils by spark cutting to minimize deformation. The samples were electrochemically thinned in polishing equipment at room temperature in a solution of 49% methanol, 49% nitric acid and 2% hydrochloric acid.

4. Results and Discussion

4.1. Mean Jump Distance of Moving Dislocations in Al

As described by Eq. (2), from the magnitude of the slope of the curve $(T_{1\rho}^{-1})_D$ vs $\dot{\varepsilon}$ the mean jump distance L can be obtained provided the other parameters are known. The strain dependence of L has been obtained from measuring $T_{1\rho}^{-1}$ as a function of ε. The results are depicted in Fig. 1. It has to be emphasized that the mean jump distance L measured by NMR in pure Al has to be interpreted with care in terms of the mean slip distance and statistical slip length (Λ_{st}). As commonly found in annealed f.c.c. metals and in alloys, a cell structure is developed in Al after deformation at 77 K. As a result, the mean slip distance of dislocations is mainly determined by the cell size when the cell structure is well developed. Consequently, the slip length will be much larger than the mean jump distance measured by NMR (0.09 µm for $\varepsilon > 7\%$). To explain this difference, it has to be realized that all moving dislocations, present both in the cell boundary and in the interior region of the cell, affect the spin-lattice relaxation

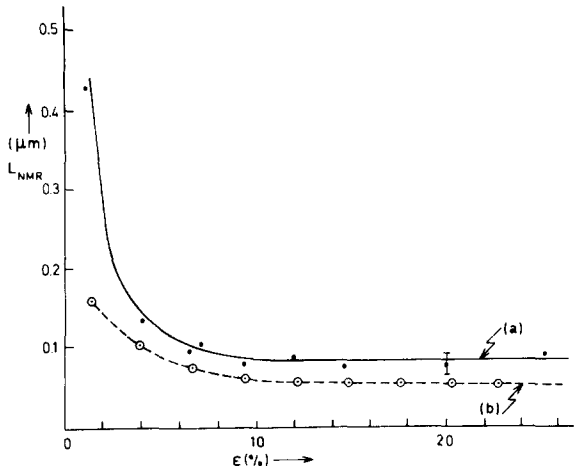

FIG. 1: The mean jump distance measured by NMR as a function of strain in (a) ultra pure Al and in (b) Al-1 at% Zn. Each data point represents the average value over 5 measurements. The error bar indicates the deviation within a set of L data at a particular ε ($\dot{\varepsilon}$ = 1.6 s^{-1}, T = 77 K).

rate. Assuming two different sets of corresponding mobile dislocation densities, ρ_1 in the interior of the cell and ρ_2 inside the cell wall, the total spin lattice relaxation rate can be written as:

$$\left(\frac{1}{T_{1\rho}}\right)_D = \left(\frac{1}{T_{1\rho}}\right)^{(1)} + \left(\frac{1}{T_{1\rho}}\right)^{(2)} , \tag{3}$$

where

$$\left(\frac{1}{T_{1\rho}}\right)^{(1)} \sim \frac{\rho_1}{L_{1\rho}} \quad \text{and} \quad \left(\frac{1}{T_{1\rho}}\right)^{(2)} \sim \frac{\rho_2}{L_{2\rho}} ,$$

and $\rho_1 + \rho_2 = \rho$. Since $L_1 >> L_2$, the total spin-lattice relaxation rate measured by NMR is largely determined by the jump distance inside the cell wall. The mean jump distance of dislocations measured by NMR is therefore related to the spacing of the forest dislocation tangles in the cell boundary. At the beginning of deformation the storage of dislocations follows strictly geometrical or statistical rules. If the mean jump distance is proportional to the mean slip distance (or slip line length) which decreases with increasing strain in pure f.c.c. metals, it means that

$$\frac{1}{L} \sim \dot{\varepsilon} . \tag{4}$$

From Fig. 1 we find indeed that the inverse of the mean jump distance varies linearly with strain according to Eq. (4).

To investigate whether the observed mean jump distance has the right order of magnitude, we consider forest dislocations as relatively weak localized obstacles for dislocation motion, i.e. the dislocation bends through a large angle ϕ_c in its vicinity. Assuming Friedel statistics (8), the effective obstacle spacing λ_e can be related to the average inter-obstacle spacing λ according to:

$$\lambda_e = \frac{\lambda}{\sqrt{f}} = \left(\frac{\mu b}{\tau_1 \lambda}\right)^{1/3} \lambda \tag{5}$$

where f is a measure of the obstacle strength (= $\cos \phi_c$). On the other hand the effective flow stress can be written as

$$\tau_1 = \alpha \mu b \sqrt{\rho_F} , \tag{6}$$

i.e. the applied stress diminished by the athermal forest resistance and the interplane resistance. Although there exists some dispute concerning Eq.(6), whether the flow stress is controlled by interaction between primaries or forest dislocation density ρ_F, experimental work suggests that the flow stress in pure f.c.c. in stage II is controlled by forest dislocations or that forest contributions are always in a constant ratio independent of the dislocation distribution (9). The experimental value of α for aluminium is 0.16 (10) assuming that the flow stress is fully controlled by dislocation intersections with forest

dislocations. From Eq. (6) and Eq. (5) follows $f = \alpha^{2/3} = 0.295$ taking $\lambda \simeq \rho_F^{-1/2}$. In our samples, the flow stress was found to increase from the yield stress of 10 MPa to 79 MPa at $\varepsilon = 10\%$. The effective obstacle spacing λ_e (Eqs. (5)(6))is predicted to be proportional to $1/\tau_1$. Hence, λ_e is expected to decrease by a factor of 8. Indeed, this has been confirmed by the NMR measurements: at the beginning of deformation L_{NMR} was found to be 0.7 μm decreasing to 0.09 μm at $\varepsilon = 10\%$.

4.2. Mean Jump Distance of Moving Dislocations in Al-1 at% Zn.

In Fig. 1 the mean jump distance measured by NMR in Al- 1 at% Zn is illustrated as a function of strain. The spin-lattice relaxation rate was determined at a constant strain rate $\dot{\varepsilon} = 1.6\ s^{-1}$. The shape of the L vs ε curve is quite similar to the curve obtained for ultrapure Al. The mean jump distance L at the beginning of deformation is somewhat smaller in the alloy compared to ultra pure aluminium. This can be expected since there exists an increase of the flow stress caused by the solute atoms. This increase τ_2 was found to be 0.5 MPa.

Again with Friedel statistics as a starting point, the increase of the flow stress can be written analogous to Eq. (6):

$$\tau_2 = f_2^{3/2} \frac{\mu b}{l} \quad , \tag{7}$$

where l is the mean spacing of neighbouring atoms above or below the glide plane:

$$l = \frac{b}{\sqrt{2c}} \quad . \tag{8}$$

In this local-force model, only those solute atoms in the two planes immediately adjacent to the slip plane contribute. Substituting 0.5 MPa for τ_2 and c = 0.01, the obstacle strength f_2 is calculated to be 0.003. This indicates that forest dislocations are strong obstacles compared to solute atoms. Analogous to Eq. (5), the effective obstacle spacing can be written as:

$$l_e = \frac{b}{\sqrt{2 f_2 c}} = 0.04\ \mu m. \tag{9}$$

A plausible connection between λ_e (effective forest dislocation spacing), l_e and the measured jump distance L_{NMR} can be based on the following model: all moving dislocations in the alloy, delayed at intersections with either forest dislocations or solute atoms, affect the spin-lattice relaxation rate. Assuming two different sets of corresponding mobile dislocation densities, ρ_1 and ρ_2, respectively, the total spin-lattice relaxation rate can be decomposed into two contributions analogous to Eq. (3). One can envision that at the yield stress level for the case of the dilute alloy a small fraction of the mobile primary dislocations must move through the weak obstacle field presented by the solutes before encountering forest dislocations; the effective solute spacing is much smaller than the forest dislocation spacing. The mean jump distance L_{NMR} can be written as:

$$\frac{1}{L_{NMR}} \simeq \frac{\rho_1}{\lambda_e \rho} + \frac{\rho_2}{l_e \rho} \quad . \tag{10}$$

In order to verify this expression we have to make the necessary assumption that the dislocation microstructure is the same in ultra pure aluminium and in the dilute Al-1 at% Zn alloy at a certain value of ε. In view of the method of analyzing strain-rate change experiments by Van Den Beukel and co-workers (11), this implies that a plot of $1/L_{NMR}$ vs $1/L_{NMR}$ of ultra pure aluminium is a straight line with a slope equal to one. For the alloy it will have an intercept with the ordinate of magnitude $1/l_e$ whereas for ultra pure aluminium this line will go through the origin. In fig. 2 $1/L_{NMR}$ vs $1/L_{NMR}$ ultra pure Al is depicted for both the alloy and the pure material. The value of l_e found from the intercept is equal to 0.25 μm. From a comparison between this experimental finding and the value predicted using Friedel statistics (Eq. (9)), it can be concluded that actually in each dislocation jump a number of effective solute atoms (order of 10) are bypassed. In steady state, Friedel statistics assume that a dislocation released at one obstacle must, on average, pick up exactly one. This seems to be in conflict with the experimental results obtained.

Applying Mott-Nabarro statistics (2) as a different approach, we find that the effective obstacle spacing is described by:

$$l_e = \left(\frac{4\mu b}{\tau_i l}\right)^{2/3} l \quad , \tag{11}$$

where the maximum internal stress averaged over the space of radius l/2 around each solute is :

$$\tau_i \simeq \mu \, |\delta| \, c \, \ln (1/c) \quad . \tag{12}$$

δ represents the misfit parameter ($\simeq$ 0.02) and in the localized-force model l is related to the atomic-fraction concentration c of solute by equation (8). From equation (11) l_e, the effective obstacle spacing, is calculated to be 0.15 μm which is in reasonable agreement with the experimental indication of 0.25 μm. (Fig. 2).

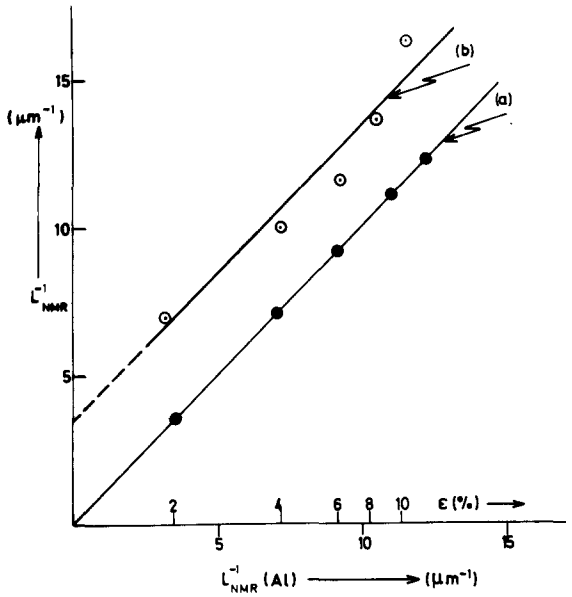

FIG. 2: Inverse mean jump distance L_{NMR} vs the same quantity of L_{NMR} in ultra pure aluminium.
(a): Ultra pure Al, (b): Al-1 at% Zn.

According to our assumption, l_e is the effective spacing between solute atoms and is independent of strain. Furthermore, λ_e is the effective separation of forest dislocations in the solid without solute atoms and has the same strain dependence in the alloy as in the ultra pure material. To verify equation (10) we set λ_e equal to the value found in ultra pure aluminium ($\simeq$ 0.7 μm) and take for l_e the predicted value of 0.15 μm. Further, the two different fractions of mobile dislocation densities in Eq. (10) are assumed to be proportional to the corresponding ratio's of the effective planar obstacle densities.

At the beginning of deformation L_{NMR} is predicted to be 0.16 μm according to

$$\frac{1}{L_{NMR}} = \frac{0.04}{\lambda_e} + \frac{0.96}{l_e} \quad , \tag{13}$$

which is in agreement with experimental observations (Fig. 1). At higher deformation L_{NMR} in the alloy will approach λ_e as found in the ultra pure material. At higher deformation the ratio of the effective obstacle densities, solutes and forest dislocations lowers probably only by a factor of 10 leading to a higher value of L_{NMR} in the alloy than in the ultra pure material. However, just the opposite has been observed (Fig. 1). This can be explained as follows: when primaries move through a random field of solute atoms before encountering forest dislocations, the dislocation mobility is decreased relative to that possible at the same stress level compared to a ultra pure material. In order to keep up with a fixed applied strain rate $\dot{\varepsilon}$ (Eq. (1)), the dilute alloy may have ρ_m greater than for the pure crystal. Consequently, at a corresponding strain the alloy has to have a higher stress level than the ultra pure crystal. It means that the effective obstacle spacing λ_e (Eq. (5)) in the alloy at higher deformation stages can become smaller than λ_e observed in the ultra pure material. This discussion ignores the effect of solutes on the stacking fault energy of aluminium (cell structure formation). Nevertheless, TEM observations of the present dilute alloy system show a cell structure quite similar to the structure found in ultra pure Al (see Fig. 3).

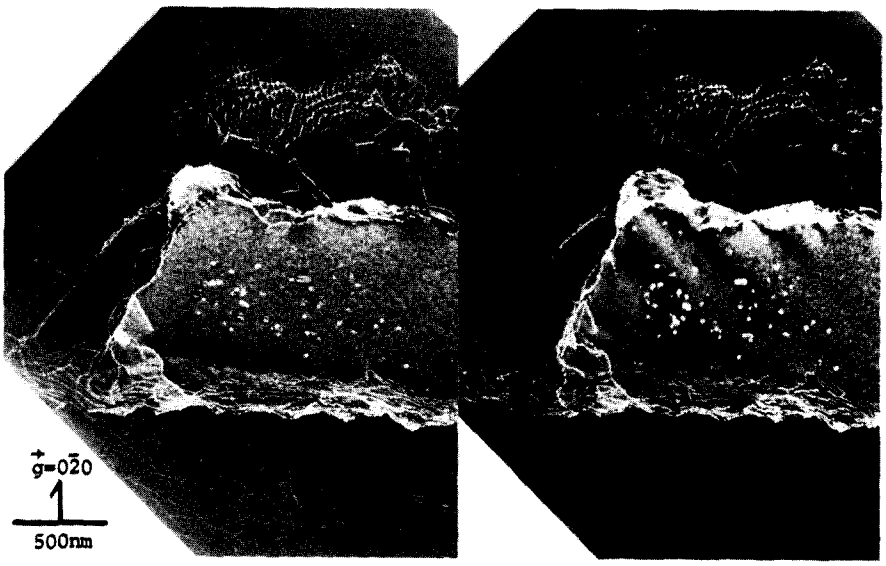

FIG. 3: Stereo-electron micrograph of Al:1 at% Zn, deformed at 77 K until fracture, $\mathbf{g} = 0\bar{2}0$, stereo angle 22°, stereo impression [201].

5. Conclusion

Pulsed nuclear magnetic resonance is shown to be a complementary new technique for the study of moving dislocations in Al-Zn alloys. Spin-lattice relaxation measurements clearly indicate that fluctuations in the quadrupolar field caused by moving dislocations in Al-Zn are different than those in ultra pure Al. The mean jump distance found in ultra pure Al can be explained using Friedel statistics for describing the interaction between moving dislocations and forest dislocations. In the alloy system a combination of both Mott-Nabarro statistics for the interaction with solute atoms and Friedel statistics for the interaction with forest dislocations has been applied. In fact, only fairly strong obstacles at very low concentrations ($c \approx 10^{-3}$) seem to fall inside the range where Friedel statistics are justified. Forest dislocations are probably a borderline case. In contrast, Labusch (12), presenting a more complete solution of the statistical problem of hardening, finds that Friedel statistics are rarely justified.

Acknowledgement

The work is part of the research program of the Foundation for Fundamental Research on Matter (F.O.M.-Utrecht) and has been made possible by financial support from the Netherlands organization for the Advancement of Pure Research (Z.W.O.-The Hague) and the Deutsche Forschungsgemeinschaft, FRG.

References

1. E. Orowan, Z. Phys. **89**, 634 (1934).
2. F. R. N. Nabarro, in: The Physics of Metals: 2 Defects, P. B. Hirsch, ed., Cambridge Un.Press, p. 152,1975.
3. F. R. N. Nabarro, Phil. Mag. **35**, 613 (1977).
4. J. Th. M. De Hosson, O. Kanert, A. W. Sleeswyk, in: Dislocations in Solids, F. R. N. Nabarro, ed., Vol. **6**, pp 441-534 (1983), North Holland, Amsterdam.
5. H. J. Hackelöer, O. Kanert, H. Tamler, J. Th. M. De Hosson, Rev. Sci. Instr. **54**, 341 (1983).
6. A. D. Le Claire, J. of Nuclear Materials **69&70**, 70 (1978).
7. N. L. Peterson, J. of Nuclear Materials **69&70**, 3 (1978).
8. U. F. Kocks, A. S. Argon, M. F. Ashby, Progress in Materials Science, Vol. **19**, pp. 40 (1975).
9. P. B. Hirsch, in: The Physics of Metals: 2 Defects, P. B. Hirsch, ed., Cambridge Un. Press, p. 189, 1975.
10. Z. S. Basinski, Phil. Mag. **40**, 393 (1959).
11. G. J. Den Otter and A. van den Beukel, Phys. Stat. Sol. (a) **55**, 785 (1979).
12. R. Labusch, Acta Metall. **20**, 917 (1972).